Thermal Radiative Properties of Nanoscale Semiconductors with Incoherent Formulation

Seyed Amir Abbas Oloomi*
Department of Mechanical Engineering,
Isfahan University of Technology, Isfahan, Iran
E-mail: Amiroloomi@me.iut.ac.ir
*Corresponding author

Ahmad Saboonchi
Department of Mechanical Engineering,
Isfahan University of Technology, Isfahan, Iran
E-mail: AhmadSab@cc.iut.ac.ir

Ahmad Sedaghat
Department of Mechanical Engineering,
Isfahan University of Technology, Isfahan, Iran
E-mail: Sedaghat@cc.iut.ac.ir

Archive of SID

Abstract: Rapid thermal processing (RTP) has become a key technology for semiconductor device manufacturing in a variety of applications, such as thermal oxidation, annealing, and thin-film growth. Hence, understanding the radiative properties of silicon and other relevant materials is essential for the analysis of the thermal transport processes. We have analyzed and calculated the spectral, directional and temperature dependency of radiative properties of a three layers material using transfer-matrix method. In the present work empirical expressions for calculating the optical constants of materials are carefully selected. The studied examples using silicon wafer and either silicon dioxide or silicon nitride coating demonstrate the strong influence of coating and coating thickness on the radiative properties. This study helps to gain a better understanding of the radiative properties of semitransparent wafers with different coatings and will have an impact not only on semiconductor processing but also on thin film solar cells. Results showed that silicon dioxide coating has higher reflectance than silicon nitride coating for visible wavelengths. Therefore coatings act as wavelength selective emitters for radiative energy conversion and thermal radiation detection. In visible wavelengths the reflectance increases as the temperature increases, because of decreasing emittance but in infrared wavelengths the reflectance and transmittance decrease as the temperature increases. The layer thicknesses need to be optimized to achieve maximum transmittance for the given materials. Maximum transmittance also depends on the type of materials and its temperature.

Keywords: Incoherent Formulation- Nano scale- Properties- Semiconductor- Thermal Radiative

Reference: Oloomi, S. A. A., Saboonchi, A., Sedaghat, A., "Thermal Radiative Properties of Nanoscale Semiconductors with Incoherent Formulation", Majlesi Journal of Mechanical Engineering, Vol. 3, No. 2, 2010, pp. 45–52.

Biographical notes: S. A. A. Oloomi is currently PhD Student in mechanical engineering at Isfahan University of Technology. His current research interest includes nanosclae radiative properties and trigeneration systems. **A. Saboonchi** is Associate Professor of mechanical engineering at the Isfahan University of Technology, Iran. He received his PhD in mechanical engineering from Okla University, USA. His current research focuses on heat transfer. **A. Sedaghat** is Assistant Professor of mechanical engineering on aerospace at the Isfahan University of Technology, Iran. He received his PhD in aerospace engineering from The University of Manchester, UK. His current research focuses on aerodynamics, hydrodynamics and CFD.

© 2010 IAU, Majlesi Branch

www.SID.ir

1 INTRODUCTION

Radiative properties of a material are the core of thermal science and optics, which play critical roles in modern technologies, including MEMS/NEMS. The radiative properties, such as reflectance, transmittance, and emittance of multilayer structures largely depend on the direction and wavelength of incident radiation as well as wafer temperature. They are also affected by thin-film coatings and surface roughness [1].

The studied examples using silicon wafer and either silicon dioxide or silicon nitride coating demonstrate the strong influence of coating and coating thickness on the radiative properties. This study helps to gain a better understanding of the radiative properties of semitransparent wafers with different coatings and will have an impact not only on semiconductor processing but also on thin film solar cells.

Fu studied radiative properties of NIMs by using three multilayer structures with NIM layer [1]. We have interested in studying nanoscale radiative properties with silicon because silicon is the most extensively used material in MEMS/NEMS.

During the past two decades, there have been tremendous developments in near-field imaging and local probing techniques. Examples are the Scanning Tunneling Microscope (STM), Atomic Force Microscope (AFM), Near-field Scanning Optical Microscope (NSOM), Photon Scanning Tunneling Microscope (PSTM), and Scanning Thermal Microscope (SThM).

The ability to manufacture, control, and manipulate structures at extremely small scales is the hallmark of modern technologies, which include microelectronics, MEMS/NEMS, and nanobiotechnology. Spectral and directional control of thermal radiation is a challenging yet important task for a number of applications, such as thermophotovoltaic (TPV) energy conversion, solar energy utilization, space thermal management, and high-efficiency incandescent lamps.

Pattern-induced radiative property variations can be an important problem for the wafer temperature measurement and the temperature uniformity control during integrated circuit manufacturing. In addition, light diffraction can be used to monitor the etching depth and other features during the microfabrication and lithographic processes.

Heat transfer at nanoscale may differ significantly from that in macroscales. With device or structure characteristic length scales becoming comparable to the mean free path and wavelength of heat carriers (electrons, photons, phonons, and molecules), classical laws are no longer valid and new approaches must be taken to predict heat transfer at nanoscale.

Rapid thermal processing (RTP) has become a key technology for semiconductor device manufacturing in a variety of applications, such as thermal oxidation, annealing, and thin-film growth. Temperature measurements and control are critically important for continuous improvement of RTP [2, 3]. Since the heating source is at a much higher temperature than that of the silicon wafer, radiative energy exchange is the dominant mode of heat transfer. Hence, understanding the radiative properties of silicon and other relevant materials is essential for the analysis of the thermal transport processes. Furthermore, since many RTP furnaces use noncontact lightpipe thermometers, accurate determination of the wafer emittance is necessary for correlating the radiance temperature to the true wafer temperature [4, 5]

This Paper, predicts the directional, spectral, and temperature dependence of the radiative properties for the multilayer structures consisting of silicon and related materials such as silicon dioxide, and silicon nitride.

2 MODELING

2.1. Coherent Formulation

When the thickness of each layer is comparable or less than the wavelength of electromagnetic waves, the wave interference effects inside each layer become important to correctly predict the radiative properties of multilayer structure of thin films. The transfer-matrix method provides a convenient way to calculate the radiative properties of multilayer structures of thin films (Figure 1).

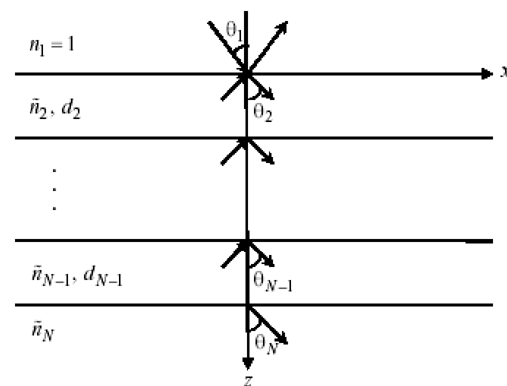

Fig. 1 The geometry for calculating the radiative properties of a multilayer structure

By assuming that the electromagnetic field in the *j*th medium is a summation of forward and backward waves in the *z*-direction, the electromagnetic field in each layer can be expressed by

$$E_j = \begin{cases} \left[A_1 e^{iq_{1z}z} + B_1 e^{-q_{1z}z}\right] e^{(iq_x x - i\omega t)}, \ j=1 \\ \left[A_j e^{iq_{jz}(z-z_{j-1})} + B_j e^{-q_{jz}(z-z_{j-1})}\right] e^{(iq_x x - i\omega t)}, \ j=2,3,...N \end{cases} \quad (1)$$

© 2010 IAU, Majlesi Branch

www.SID.ir

Where A_j and B_j are the amplitudes of forward and backward waves in the jth layer. Detailed descriptions of how to solve for A_j and B_j is given in [1].

2.2. Incoherent Formulation

When the thickness of silicon substrate is much greater than the coherent length, and the considered wavelength falls in the semitransparent region of silicon, interferences in the substrate are generally not observable from the measurements. In this case, the incoherent formulation or geometric optics should be used to predict the radiative properties of the silicon substrate. Two ways to get around this problem are to use the fringe-averaged radiative properties and to treat thin-film coatings as coherent but the substrate as incoherent [1] (Figure 2).

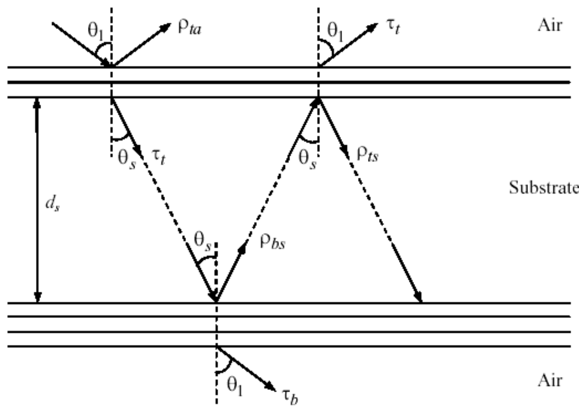

Fig. 2 Schematic of thin-film coatings on both sides of a thick silicon

Figure 2 shows the geometry of the silicon wafer with thin-film coatings on both sides. Note that ρ_{ta} and τ_t are the reflectance and transmittance, respectively, of the multilayer structure at the top surface (air- coatings- silicon) for rays incident from air, assuming that the silicon extends to infinite. On the other hand, ρ_{ts} and τ_b are for rays incident from silicon. Note that the transmittance τ_t is the same when absorption inside silicon is negligibly small [6]. Similarly, ρ_{bs} and τ_b are for the multilayer structure at the bottom surface for rays incident from the substrate. The transfer-matrix method can be separately applied to calculate the reflectance and transmittance at the top and bottom surfaces of the wafer, by neglecting the absorption of silicon. The absorption of silicon can be taken into consideration by introducing the internal transmittance

$$\tau_i = \exp(-\frac{4\pi k_s d_s}{\lambda \cos\theta_s}) \tag{2}$$

Here, k_s is the extinction coefficient of silicon, d_s is the thickness, and θ_s is the angle of refraction. The angle of refraction is complex due to absorption.

For a slightly absorbing medium with $k_s \prec\prec 1$, however, θ_s can be determined using Snell's law by neglecting absorption [7]. Consequently, the radiative properties of the silicon wafer with thin-film coatings in the semitransparent region can be expressed as [8].

$$\rho = \rho_{ta} + \frac{\tau_i^2 \tau_t^2 \rho_{bs}}{1-\tau_i^2 \rho_{ts}\rho_{bs}} \tag{3}$$

$$\tau = \frac{\tau_i\, \tau_t\, \tau_b}{1-\tau_i^2 \rho_{ts}\rho_{bs}} \tag{4}$$

$$\varepsilon = 1-\rho-\tau \tag{5}$$

3 OPTICAL CONSTANTS

The optical constants, including the refractive index (n) and the extinction coefficient (κ), of a material are complicated functions of the wavelength and temperature. They also depend on the crystalline structure as well as doping and impurity levels. In the present work, carefully selected empirical expressions are used to calculate the optical constants of lightly doped silicon (doping concentration $<10^{15} cm^{-3}$).

3.1. The Refractive Index of Silicon

Jellison and Modine measured the ratio of the Fresnel reflection coefficients of silicon wafers in both polarization states with a two-channel spectroscopic ellipsometer in the temperature range from 25 °C to 490 °C [10]. From the measurement results, they extracted the refractive index and extinction coefficient using the least-squares Levenberg-Marquardt fitting.

The Jellison and Modine (J-M) expression of the refractive index for wavelength between 0.4 µm and 0.84 µm is given by

$$n_{JM}(\lambda, T) = n_0(\lambda) + \beta(\lambda)T \tag{6}$$

$$n_0 = \sqrt{4.565 + \frac{97.3}{3.648^2 - (1.24/\lambda)^2}} \tag{7}$$

$$\beta(\lambda) = -1.864\times10^{-4} + \frac{5.394\times10^{-3}}{3.648^2 - (1.24/\lambda)^2} \tag{8}$$

where $\lambda[\mu m]$ is the wavelength in vacuum and T [°C] is the temperature. Li extensively reviewed the refractive index of silicon [3]. By carefully analyzing published experimental data, he developed a functional relation, based on the modified Sell Meier type dispersion relation, for the refractive index of silicon that covers the wavelength region between 1.2 µm and 14 µm and the temperature range up to 480 °C.

Archive of SID

© 2010 IAU, Majlesi Branch

www.SID.ir

$$n_L(\lambda,T)=\sqrt{\varepsilon_r(T)+\frac{g(T)\eta(T)}{\lambda^2}} \quad (9)$$

$$\varepsilon_r(T)=11.631+1.0268\times10^{-3}T+ 1.0384\times10^{-6}T^2-8.1347\times10^{-10}T^3 \quad (10)$$

$$g(T)=1.0204+4.8011\times10^{-4}T+7.3835\times10^{-8}T^2 \quad (11)$$

$$\eta(T)=\exp(1.786\times10^{-4}-8.526\times10^{-6}T -4.685\times10^{-9}T^2+1.363\times10^{-12}T^3) \quad (12)$$

To calculate the refractive index of silicon, in this study the J-M expression is used in the wavelength region from 0.5 µm to 0.84 µm, and Li's expression at wavelengths above 1.2 µm. In the wavelength range between 0.84 µm and 1.2 µm, we use a weighted average based on the extrapolation of the two expressions. Notice that beyond 6 µm or so, lattice vibration causes additional absorption; however, its effects can be neglected due to the weakness of the phonon oscillators in silicon. Figure 3 shows the calculated refractive index of silicon in the wavelength range from 0.5 µm to 10.0 µm at selected temperatures. In general, the refractive index of silicon decreases as the wavelength increases and the temperature decreases. When $\lambda > 10.0$ µm, the refractive index of Si is assumed to be independent of the wavelength, and the value of $n_L(\lambda=10,T)$ is used to represent the refractive index of Si at any temperature T for $\lambda > 10.0$ µm.

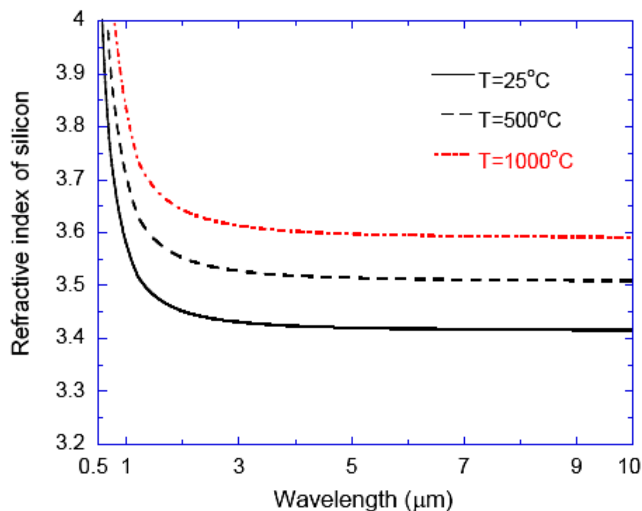

Fig. 3 Calculated refractive index of silicon at selected temperatures

3.2. The Extinction Coefficient of Silicon

The extinction coefficient (κ) and absorption coefficient (α) are related by $\alpha=4\pi k/\lambda$. The absorption coefficient of silicon depends on the absorption processes, such as interband transition, intraband transition, and free-carrier absorption. When the photon energy is higher than the band gap energy of silicon, electrons in the valance band can be excited to the conduction band, resulting in a large absorption coefficient.

The J-M expression of the extinction coefficient, covering the wavelength range from 0.4 µm to 0.84 µm, is given as [10]:

$$k_{JM}(\lambda,T)=k_0(\lambda)\exp\left[\frac{T}{369.9-\exp(-12.92+6.831/\lambda)}\right]$$

$$k_0(\lambda)=-0.0805+\exp\left[-3.1893+\frac{7.946}{3.648^2-(1.24/\lambda)^2}\right]$$

The absorption coefficient can be deduced from the extinction coefficient. In the longer wavelength region, Timans measured the emission spectra of several silicon wafers and deduced the absorption coefficient in the wavelength region from 1.1 µm to 1.6 µm, in the temperature range between 330°C and 800°C [8]. He suggested that the absorption coefficient can be expressed as a summation of the band gap absorption and free-carrier absorption as following:

$$\alpha(\lambda,T)=\alpha_{BG}(\lambda,T)+\alpha_{FC}(\lambda,T) \quad (13)$$

The expression for the band gap absorption can be found in the work by MacFalane et al. [11] and is given by

$$\alpha_{BG}(\lambda,T)=\sum_{i=1}^{4}\alpha_{a,i}(\lambda,T)+\sum_{i=1}^{2}\alpha_{e,i}(\lambda,T) \quad (14)$$

Notice that silicon is an indirect-gap semiconductor and the absorption process is accompanied by either the absorption of a phonon, denoted by $\alpha_{a,i}(\lambda,T)$, or the emission of a phonon, denoted by $\alpha_{e,i}(\lambda,T)$. Detailed expressions for $\alpha_{a,i}(\lambda,T)$ and $\alpha_{e,i}(\lambda,T)$ can be found in Timans [8, 12]. The band-gap absorption disappears at wavelengths longer than that corresponding to the energy gap (modified by the phonon energy). For the free-carrier absorption, Sturm and Reaves suggested an expression based on their measurement of the transmission of the wafer at 1.30 µm and 1.55 µm and in the temperature range of 500 °C to 800 °C [13]. The Sturm and Reaves (S-R) expression is

$$\alpha_{FC}=N_eA_e+N_hA_h \quad (15)$$

Where N_e and N_h are electron and hole concentrations, and A_e and A_h are electron and hole absorption cross sections, respectively. The S-R expression agrees well with experimental results in the wavelength region between 1.0 µm and 1.5 µm, but departs from experiments at longer wavelengths. Vandenabeele and Maex studied the free-carrier absorption of silicon in the infrared region by measuring the emission from the double-side-polished silicon wafers at the wavelengths of 1.7 µm and 3.4 µm, in the temperature range from 400 °C to 700 °C [14]. They proposed a semi-empirical relation for calculating the

© 2010 IAU, Majlesi Branch

www.SID.ir

extinction coefficient as functions of wavelength and temperature due to free-carrier absorption.

The Vandenabeele and Maex (V-M) expression is given by

$$\alpha_{FC}(\lambda,T) = 4.15\times10^{-5}\lambda^{1.51}(T+273.15)^{2.95}\exp\left(\frac{-7000}{T+273.15}\right) \tag{16}$$

Here again, T is in °C. Rogne et al. demonstrated that the absorption coefficient calculated from the V-M expression agrees well with experimental data in the wavelength region between 1.0 µm and 9.0 µm at elevated temperatures [15]. In the wavelength region between 6.0 µm and 25.0 µm, lattice vibrations causes an additional absorption. Since the effect of lattice absorption is negligible in most RTP applications compared to the absorption by free carriers, it is assumed to be independent of the temperature and dopant concentration. The extinction coefficient for lightly doped silicon due to the lattice absorption is simply obtained from the tabulated extinction coefficient values given in Ref. [16] at room temperature. The absorption coefficient of lightly doped silicon is determined from the JM expression at $\lambda <$ 0.9 µm and the Timans expression is combined with V-M expression for the free-carrier absorption at $\lambda >$ 0.9 µm. Figure 3 shows the calculated extinction coefficient of silicon in the wavelength range from 0.5 µm to 9.0 µm at selected temperatures. Notice that unlike the refractive index of silicon, there exists a discontinuity in the calculated extinction coefficient especially at the elevated temperatures because the functional expression is changed at λ=0.9 µm. The existence of the absorption edge is clearly seen from the figure, and the extinction coefficient generally increases as the temperature increases. Since the V-M expression is applicable up to 9.0 µm, the empirical models for the extinction coefficient of lightly doped silicon are inevitably limited to the wavelengths less than 9.0 µm.

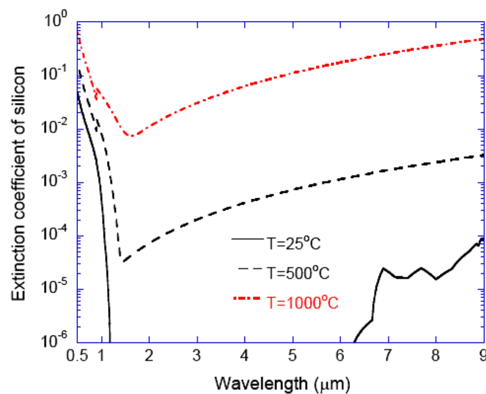

Fig. 4 Calculated extinction coefficient of silicon at selected temperatures

The optical constants of silicon dioxide and silicon nitride are mainly based on the data collected in Palik's handbook and are assumed to be independent of temperature [17, 18].

4 RESULTS

Consider the case in which the silicon wafer is coated with a silicon dioxide layer on both sides. The thickness of silicon wafer is 500 μm and the temperature of silicon wafer with thin-film coatings is 25ºC and the Electromagnetic waves are incident at $\theta = 0^\circ$. The considered wavelength range is $0.5\mu m < \lambda < 2\mu m$. $0.5\mu m < \lambda < 0.7\mu m$ is visible wavelength and $0.7\mu m < \lambda < 2\mu m$ is infrared wavelength. Some results of this study are shown below in figures 5 to 13.

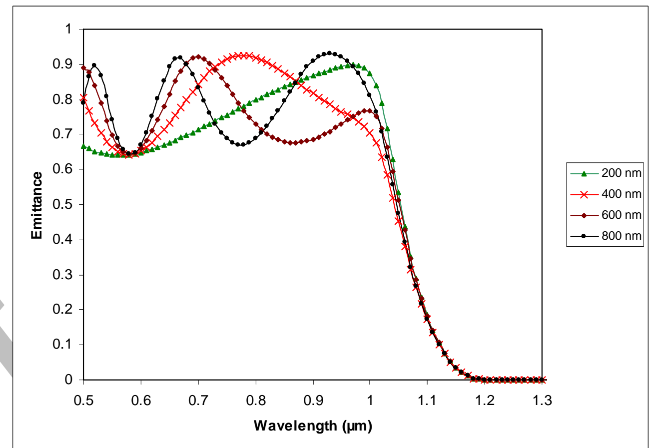

Fig. 5 Spectral emittance of silicon wafer coated with silicon dioxide film with different thicknesses (200 nm, 400nm, 600nm, 800nm) on both sides, at room Temperatures and normal incidence with Incoherent Formulation.

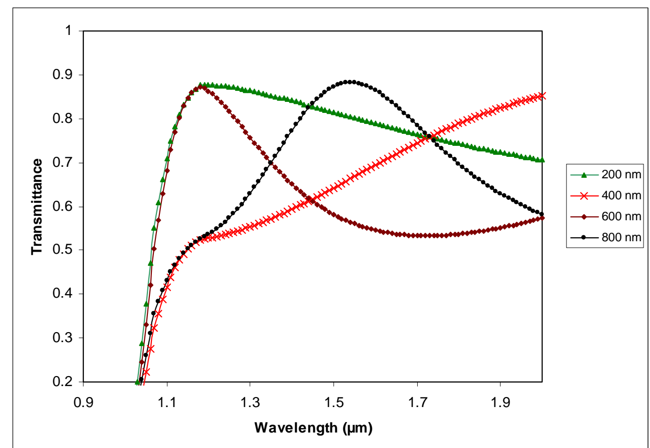

Fig. 6 Spectral transmittance of silicon wafer coated with silicon dioxide film with different thicknesses (200 nm, 400nm, 600nm, 800nm) on both sides, at room Temperatures and normal incidence with Incoherent Formulation.

© 2010 IAU, Majlesi Branch

www.SID.ir

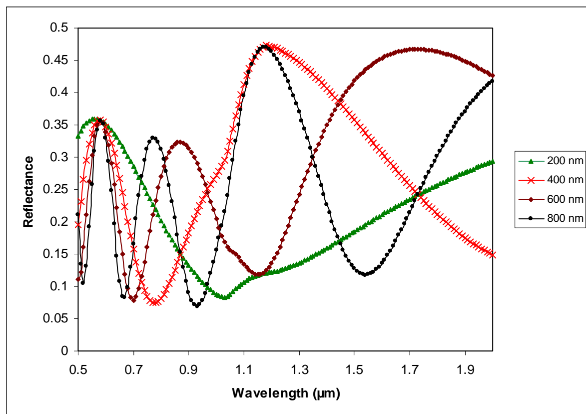

Fig. 7 Spectral reflectance of silicon wafer coated with silicon dioxide film with different thicknesses (200 nm, 400nm, 600nm, 800nm) on both sides, at room Temperatures and normal incidence with Incoherent Formulation.

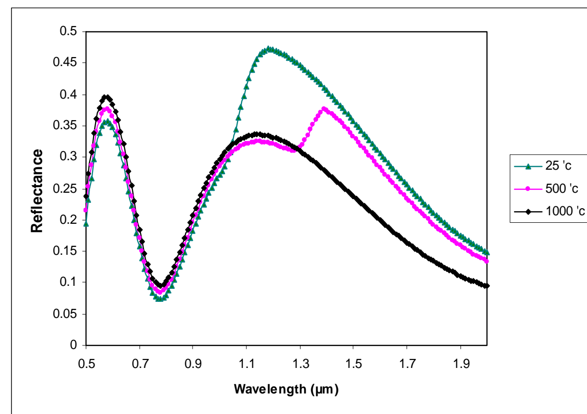

Fig. 10 Spectral reflectance of silicon wafer coated with silicon dioxide film (400 nm thickness) on both sides at different Temperatures (25°C, 500°C, 1000°C) with Incoherent Formulation.

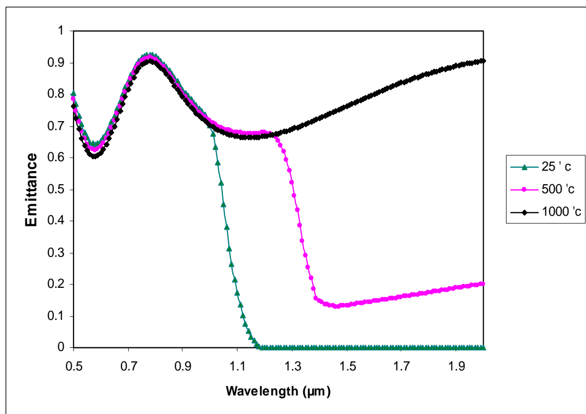

Fig. 8 Spectral emittance of silicon wafer coated with silicon dioxide film (400 nm thickness) on both sides at different Temperatures (25°C, 500°C, 1000°C) with Incoherent Formulation.

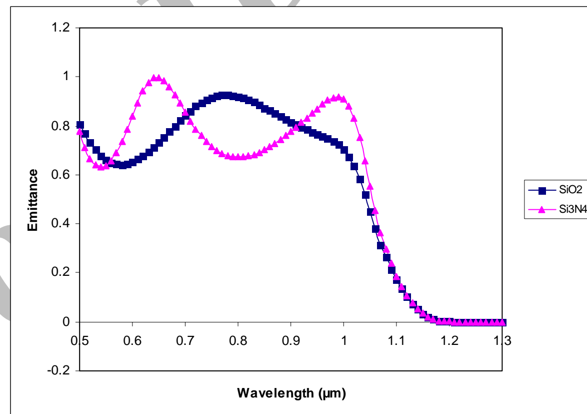

Fig. 11 Spectral emittance of silicon wafer coated with different materials (silicon dioxide and silicon nitride) on both sides (400 nm thickness), at room Temperatures and normal incidence with Incoherent Formulation.

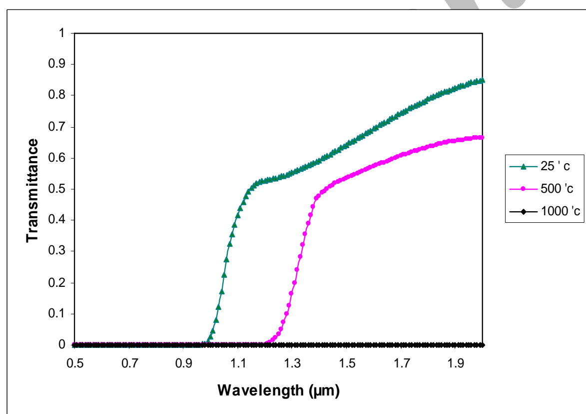

Fig. 9 Spectral transmittance of silicon wafer coated with silicon dioxide film (400 nm thickness) on both sides at different Temperatures (25°C, 500°C, 1000°C) with Incoherent Formulation.

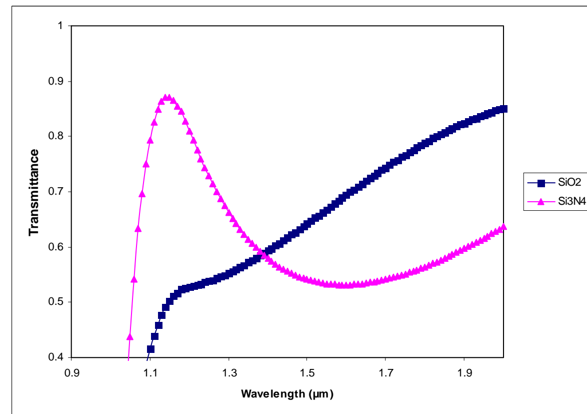

Fig. 12 Spectral transmittance of silicon wafer coated with different materials (silicon dioxide and silicon nitride) on both sides (400 nm thickness), at room Temperatures and normal incidence with Incoherent Formulation.

© 2010 IAU, Majlesi Branch

www.SID.ir

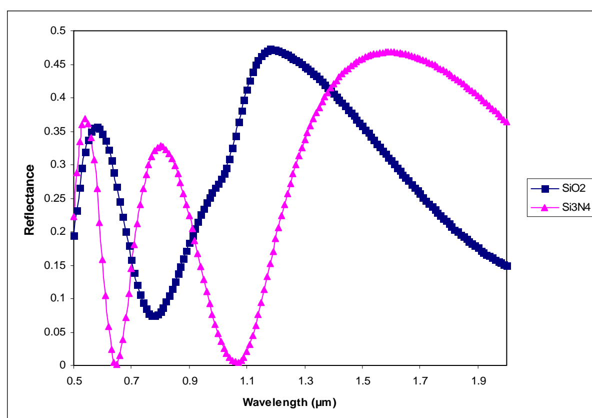

Fig. 13 Spectral reflectance of silicon wafer coated with different materials (silicon dioxide and silicon nitride) on both sides (400 nm thickness), at room Temperatures and normal incidence with Incoherent Formulation.

5 CONCLUSION

the spectral, directional and temperature dependency of radiative properties of a three layers material using transfer-matrix method are analyzed and calculated. In the present work empirical expressions for calculating the optical constants of materials are carefully selected .The layer thicknesses need to be optimized to achieve maximum transmittance for the given materials. Maximum transmittance also depends on the type of materials and its temperature.

The effect of wave interference can be understood by plotting the spectral properties such as reflectance or transmittance of a thin dielectric film versus the film thickness and analyzing the oscillations of properties due to constructive and destructive interferences [19].

Interferences in the substrate are generally not observable in Incoherent Formulation. (Figures 5 to 13) This is the major difference between coherent and incoherent Formulation.

For visible wavelengths, more emittance occurs in thicker coatings and the reflectance decreases as the coating thickness increases. In these wavelengths, transmittance is negligible.

In visible wavelengths the reflectance increases as the temperature increases, because of decreasing emittance but in infrared wavelengths the reflectance and transmittance decrease as the temperature increases.

Silicon dioxide coating has higher emittance than silicon nitride coating for $0.7\mu m < \lambda < 0.9\mu m$, but for $0.55\mu m < \lambda < 0.7\mu m$ and $0.9\mu m < \lambda < 1\mu m$ silicon nitride coating has higher emittance than silicon oxide coating. Silicon dioxide coating has higher reflectance than silicon nitride coating for visible wavelengths.

Therefore coatings act as wavelength selective emitters for radiative energy conversion and thermal radiation detection.

REFERENCES

[1] Fu, C. j, Zhang, Z. M. and Zhu, Q. Z., "Optical and Thermal Radiative Properties of Semicond uctors Related to Micro/Nanotechnology", Advanced in Heat Transfer, 37, 2003, pp. 179-296.

[2] Timans, P. J., Sharangpani, R. and Thakur, R. P. S. "Rapid Thermal Processing", Handbook of Semiconductor Manufacturing Technology, Y. Nishi and R. Doering (eds.), Marcel Dekker, Inc., New York, 2000, pp. 201-286.

[3] Zhang, Z. M., "Surface Temperature Measurement Using Optical Techniques", Annual Review of Heat Transfer, Vol. 11, C. L. Tien (ed.), Begell House, New York, 2000, pp. 351-411.

[4] Zhou, Y. H., Shen, Y. J., Zhang, Z. M., Tsai, B. K. and DeWitt, D. P., "A Monte Carlo Model for Predicting the Effective Emissivity of the Silicon Wafer in Rapid Thermal Processing Furnaces", Int. J. Heat Mass Transfer, Vol. 45, 2002, pp. 1945-1949.

[5] Tsai, B. K., DeWitt, D. P., Early, E. A., Hanssen, L. M., Mekhontsev, S. N., Rink, M., Kreider, K. G., Lee, B. J. and Zhang, Z. M., "Emittance Standards for Improved Radiaion Thermometry During Thermal Processing of Silicon Materials", 9th International Symposium on Temperature and Thermal Measurements in Industry and Science", Cavtat-Dubrovnik, Croatia, 2004.

[6] Zhang, Z. M., "Reexamination of the Transmittance Formulae of a Lamina", J. Heat Transfer, Vol. 119, 1997, pp. 645-647.

[7] Zhang, Z. M., "Optical Properties of a Slightly Absorbing Film for Oblique Incidence", Appl. Opt., Vol. 38, 1999, pp. 205-207.

[8] Timans, P. J., "The Thermal Radiative Properties of Semiconductors", Advances in Rapid Thermal and Integrated Processing, F. Roozeboon (ed.), Kluwer Academic Publishers, Dordrecht, The Netherlands, 1996, pp. 35-101.

[9] Li, H. H., "Refractive Index of Silicon and Germanium and Its Wavelength and Temperature Derivatives", J. Phys. Chem. Ref. Data, 9, 1980, pp. 561-658.

[10] Jellison, G. E. and Modine, F. A., "Optical Functions of Silicon at Elevated Temperatures", J. Appl. Phys., 76, 1994, pp. 3758-3761.

[11] Macfarlane, G. G., Mclean, T. P., Quarantine, J. E. and Roberts, V., "Fine Structure in the Absorption-Edge Spectrum of Si", Phys. Rev., Vol. 111, 1958, pp. 1245-1254.

[12] Timans, P. J., "Emissivity of Silicon at Elevated Temperatures", J. Appl. Phys., Vol. 74, 1993, pp. 6353-6364.

[13] Sturm, J. C. and Reaves, C. M., "Silicon Temperature-Measurement by Infrared Absorption - Fundamental Processes and Doping Effects", IEEE Trans. Electron Devices, Vol. 39, 1992, pp. 81-88.

[14] Vandenabeele, P. and Maex, K., "Influence of Temperature and Backside Roughness on the Emissivity of Si Wafers during Rapid Thermal-Processing", J. Appl. Phys., Vol. 72, 1992, pp. 5867-5875.

[15] Rogne, H., Timans, P. J. and Ahmed, H., "Infrared Absorption in Silicon at Elevated Temperatures", Appl. Phys. Lett., Vol. 69, 1996, pp. 2190-2192.

Archive of SID

© 2010 IAU, Majlesi Branch

www.SID.ir

[16] Edwards, D. F., "Silicon (Si)", Handbook of Optical Constants of Solids, E. D. Palik (ed.), Academic Press, Orlando, 1985, pp. 547-569.

[17] Palik, E. D., "Silicon Dioxide (SiO2)", Handbook of Optical Constants of Solids, San Diego, CA., 1998, pp. 749-763.

[18] Palik, E. D., "Silicon Nitride (Si3N4)", Handbook of Optical Constants of Solids, San Diego, CA, 1998, pp. 771-774.

[19] Oloomi, S. A. A., Sabounchi, A. and Sedaghat, A. "Predict Thermal Radiative Properties of Nanoscale Multilayer Structures", “the IASTED International Conference on Nanotechnology and Applications” , Crete-Greece, 2008.

Archive of SID

© 2010 IAU, Majlesi Branch

www.SID.ir